Journal of Hydrology 572 (2019) 671–681

Contents lists available at ScienceDirect

Journal of Hydrology

journal homepage: www.elsevier.com/locate/jhydrol

Research papers

Determining the independent impact of soil water on forest transpiration: A case study of a black locust plantation in the Loess Plateau, China

Lei Jiao[a], Nan Lu[b,c,*], Weiwei Fang[b,c], Zongshan Li[b,c], Jian Wang[b,c], Zhao Jin[a]

[a] School of Geography and Tourism, Shaanxi Normal University, Xi'an 710119, China
[b] State Key Laboratory of Urban and Regional Ecology, Research Center for Eco-Environmental Sciences, Chinese Academy of Sciences, Beijing 100085, China
[c] University of Chinese Academy of Sciences, Beijing 100049, China

ARTICLE INFO

This manuscript was handled by Marco borga, Editor-in-Chief, with the assistance of David C Le Maitre, Associate Editor

Keywords:
Soil water
Potential evapotranspiration
Evaporative demand
Transpiration
Semi-arid region

ABSTRACT

Transpiration (Tr) is influenced by environmental factors, vegetation properties, and anthropogenic management. The effect of environmental factors on Tr are taking place from two aspects: evaporative demand (i.e., potential evapotranspiration, PET) and water supply (i.e., soil water). Soil water is one of the most important factors that limit plant transpiration in terrestrial ecosystems, especially in semi-arid and arid regions. Investigating the relationship between Tr and soil water is crucial for an improved understanding of plant survival strategies and predicting hydrological cycles and water resources under climate change. Although the relationships of soil water and Tr have been widely studied, the independent effects of soil water on Tr are difficult to separate because soil water and PET occur concurrently under natural conditions. This study carried out field observations of sapflow density, meteorological factors and soil water in a black locust (*Robinia pseudoacacia*) plantation in the semi-arid Loess Plateau of China. This information was used to develop a model integrating the daily PET and relative extractable soil water (REW, an index that represents the available soil water): $Tr = (0.27 \times PET - 0.02 \times PET^2 - 0.32) \times (1 - e^{-5.70 \times REW})$. The model fitted the measured data well ($R^2 = 0.65$ and RMSE = 0.06 mm day^{-1}). We found that the daily Tr increased as the REW increased under varying PET levels. Additionally, the independent effects of soil water on Tr were analysed using the factorial experiment analysis method. The REW was manipulated and PET varied naturally during the measurements to separate the independent effects of the REW on Tr. The results showed that Tr increased with the REW during the study period at a rate of 0.53 mm day^{-1} per 0.1 REW when the REW $<$ 0.4 and 0.09 mm day^{-1} per 0.1 REW beyond the threshold (REW = 0.4). Tr increased by 27.3 mm (43.7%) compared to the controlled Tr (observed PET and lowest REW) due to the effects of increasing REW (ranging from 0.14 ~ 0.81) during the study period (growing seasons of 2015 and 2016). Furthermore, canopy-level stomatal conductance was calculated using a simplified inverted Penman-Monteith equation. The reference canopy-level stomatal conductance (Gsref), which represents the Gs capacity and its sensitivity to soil water, showed an increasing response with increasing REW, which is the possible reason for the Tr dynamics with the REW. Our study provided an improved understanding of the soil water-Tr relationship and predicted effects of climate change on tree water use. Although the method required abundant field observation data, we have provided a feasible method of accurately quantifying the independent contribution of soil water on forest Tr.

1. Introduction

Transpiration (Tr) is the process by which water is transferred from soil to the atmosphere through plants and represents the key link coupling terrestrial water cycling and energy balance (Ungar et al., 2013; Kumagai et al., 2014). On a global scale, Tr plays an important role in water balance and accounts for more than 60% of the evapotranspiration (ET) in terrestrial ecosystems (Jasechko et al., 2013). Tr is influenced by environmental factors, vegetation properties (leaf area index, tree age, density, root characteristics, etc.) and anthropogenic management (thinning, pruning) (Angstmann et al., 2012; Raz-Yaseef et al., 2012; Alcorn et al., 2013). Environmental factors have significant impacts on Tr, and these impacts have been widely studied at the leaf, tree and stand scales (Kumagai et al., 2008; Ghimire et al.,

* Corresponding author at: State Key Laboratory of Urban and Regional Ecology, Research Center for Eco-Environmental Sciences, Chinese Academy of Sciences, Beijing 100085, China.
E-mail address: nanlv@rcees.ac.cn (N. Lu).

https://doi.org/10.1016/j.jhydrol.2019.03.045
Received 6 September 2018; Received in revised form 6 March 2019; Accepted 7 March 2019
Available online 16 March 2019

2014; Shimizu et al., 2015). The environmental factors that affect Tr include soil water, air temperature, relative humidity, wind speed and solar radiation (Oren and Pataki, 2001; O'Brien et al., 2004). These factors can be divided into two aspects according to the underlying mechanisms (Naithani et al., 2012; Grossiord et al., 2017). One aspect is evaporative demand, which includes solar radiation, air temperature, relative humidity and wind speed, all of which drive the transpiration process, as well as potential evapotranspiration (PET), which is a compound index that characterizes the local meteorological and evaporative conditions (Jiao et al., 2016b; Li et al., 2017b). The other aspect is the water supply, i.e., soil water, which provides available water for plant transpiration (Naithani et al., 2012; Ungar et al., 2013). The relative extractable soil water is an index that represents the soil water available for plants (Granier et al., 1999; Granier et al., 2000). Numerous studies showed that water stress to plants occurred when REW value declined less than a threshold of 0.4 (Granier et al., 1999; MacKay et al., 2012). Ecosystem water stress is frequently characterized by the decline in soil water availability because soil water is important for plant growth and vegetation productivity (Dymond et al., 2017), especially in semi-arid and arid regions with deep groundwater levels.

Climate change is expected to induce stress on forest evaporation processes and productivity by reducing the available water due to low precipitation and warming (Allen et al., 2015), which could exert negative impacts on Tr and thus result in variations in hydrological cycling and water resources. Previous studies have consistently concluded that increased atmospheric evaporative demand promotes Tr, which can be expressed via linear or non-linear (exponential and polynomial) functions for different plants in different climatic regions (O'Brien et al., 2004; Ghimire et al., 2014; Grossiord et al., 2017). However, studies on the effects of increased soil water on Tr have not reached consistent conclusions. This is possibly related to root distribution, soil water variations and effects of climate on Tr (Kume et al., 2007; Kumagai et al., 2008; Brito et al., 2015). Several studies found that Tr increases as the soil water increases (Lagergren and Lindroth, 2002; Chang et al., 2014; Ji et al., 2016), while others found that Tr initially increases rapidly and then gradually decreases after its maximum soil water reaches a threshold, which is expressed as a polynomial function of soil water (Zhao and Liu, 2010). Several studies reported that clear relationships do not occur between Tr and soil water (Kumagai et al., 2008; Brito et al., 2015). Therefore, investigating the relationship between plant transpiration and soil water is crucial for an improved understanding of plant survival strategies and the effects of vegetation on water resources (Angstmann et al., 2013). Furthermore, to improve the predictions of plant responses to climate change and the alteration of hydrological cycles in the future, it is essential to identify the independent effects of soil water on Tr (MacKay et al., 2012; Kreuzwieser and Rennenberg, 2014), which will provided a better understanding of the variations in forest water use in water-limited regions under climate change regimes (Li et al., 2017b). However, soil water and PET occurs concurrently under natural conditions; thus, it is difficult to disentangle the independent effects of soil water under natural conditions.

To address the aforementioned problems, precipitation manipulation experiments and potted experiments have been frequently used to investigate the responses to soil water stress (Fisher et al., 2007; Poorter et al., 2012). In precipitation manipulation experiments, soil water levels can be manipulated while using a fixed atmospheric demand between different treatments. Therefore, the relative effects of atmospheric demand on Tr were eliminated. Such a method has been successfully used in different forests (rain forests, deciduous forests and coniferous forests) in various regions around the world (Fisher et al., 2007; MacKay et al., 2012; Poorter et al., 2012). However, precipitation exclusion experiments are unsuitable for forests with complex topography, which has resulted in knowledge gaps about the various responses of forests in mountainous regions. Moreover, potted experiments with plants and seedlings under experimental field conditions may not represent the true responses of mature forests (Poorter et al., 2012). Therefore, it is necessary to develop a method that examines the relationship between Tr and soil water under natural conditions to reflect the true response of plants to the single stress of soil water.

The semi-arid area in the Chinese Loess Plateau is the deepest loess deposit in the world, and it has a depth greater than 100 m (Fu et al., 2017). The groundwater level ranges from 30 m to 100 m below the surface (Yang et al., 2012; Jia et al., 2013). Plant roots cannot access the ground water; thus, soil water is the main water source for plants (Fang et al., 2017; Wang et al., 2017). Therefore, soil water in the root zone largely determines plant growth and survival in this region (Wang et al., 2017). Fang et al. (2017) found that three shrubs increased nocturnal transpiration to meet water demand under soil drought in this region. Soil erosion is the most serious environmental problem in this region (Wang et al., 2011). Black locust (*Robinia pseudoacacia*) is a deciduous tree species native to North America and one of the most ecologically important species due to its essential role in erosion reduction, soil improvement and carbon sequestration (Wang et al., 2011), and it was widely planted on the slopes of the semi-arid area in the Chinese Loess Plateau after the implementation of the "Grain for Green Programme" in 1999 (Jiao et al., 2016a). However, severe soil desiccation occurred in the black locust plantations, which exerted negative impacts on plant growth and regional water resources (Wang et al., 2010). Compared with the native *Quercus liaotungensis* and *Armeniaca sibirica*, black locust was more vulnerable to be influenced by soil water conditions (Du et al., 2011). Additionally, the temporal dynamics of soil water are markedly influenced by rainfall, resulting in a wide range of soil moisture values at the annual, monthly and daily scales, especially under climate change regimes with low precipitation (Zhang et al., 2018). Therefore, disentangling the independent effect of soil water on Tr is crucial for improving the knowledge of the adaptation of exotic plantations, which is beneficial to predict the effects of climate change on ecologically sustainable development in this water-limited region.

In this study, we conducted field observations of Tr, soil water content and meteorological factors in a black locust plantation in the semi-arid Chinese Loess Plateau. The REW was calculated based on the soil water, field capacity and wilting point in the study plantation. Subsequently, we established a model integrating the effects of PET and REW on Tr on a daily scale. Based on the model, the independent contribution of soil water on Tr was investigated using a factorial experiment method. Specifically, our objectives were to (1) develop an integrated model to describe the PET-REW-Tr relationship; and (2) investigate the independent effects of soil water on Tr.

2. Materials and methods

2.1. Site description

This study was conducted in the Yangjuangou catchment (36°24′N, 109°31′E) located in the central region of the Chinese Loess Plateau (Fig. 1a and b). The catchment is a typical loess hilly-gully region. The site is characterized by erodible calcaric cambisol soil derived from loess, and the soil depth is 50–200 m (Fig. 1c). The soil type is silty loam, which has a texture that consists of more than 50% silt (0.002–0.05 mm), < 20% clay (< 0.002 mm) and nearly 20% sand (> 0.05 mm). The vegetation consists of forests, shrubs, orchards, abandoned fields and crops. The forest is dominated by black locust plantations, which were widely planted at the beginning of 1980 s to control soil erosion. The climate is semi-arid, with a mean annual temperature of 9.8 °C and a mean annual precipitation of 531.0 mm (1952–2012). More than 58% of the rainfall is concentrated between July and September (Fig. 2). The growing season is from May to September for most deciduous plants in this region.

At the study site, a nearly 30-year-old black locust plantation was studied in the catchment. The plantation is located on the south slope aspect and the middle-slope position at an altitude of 1179 m. The

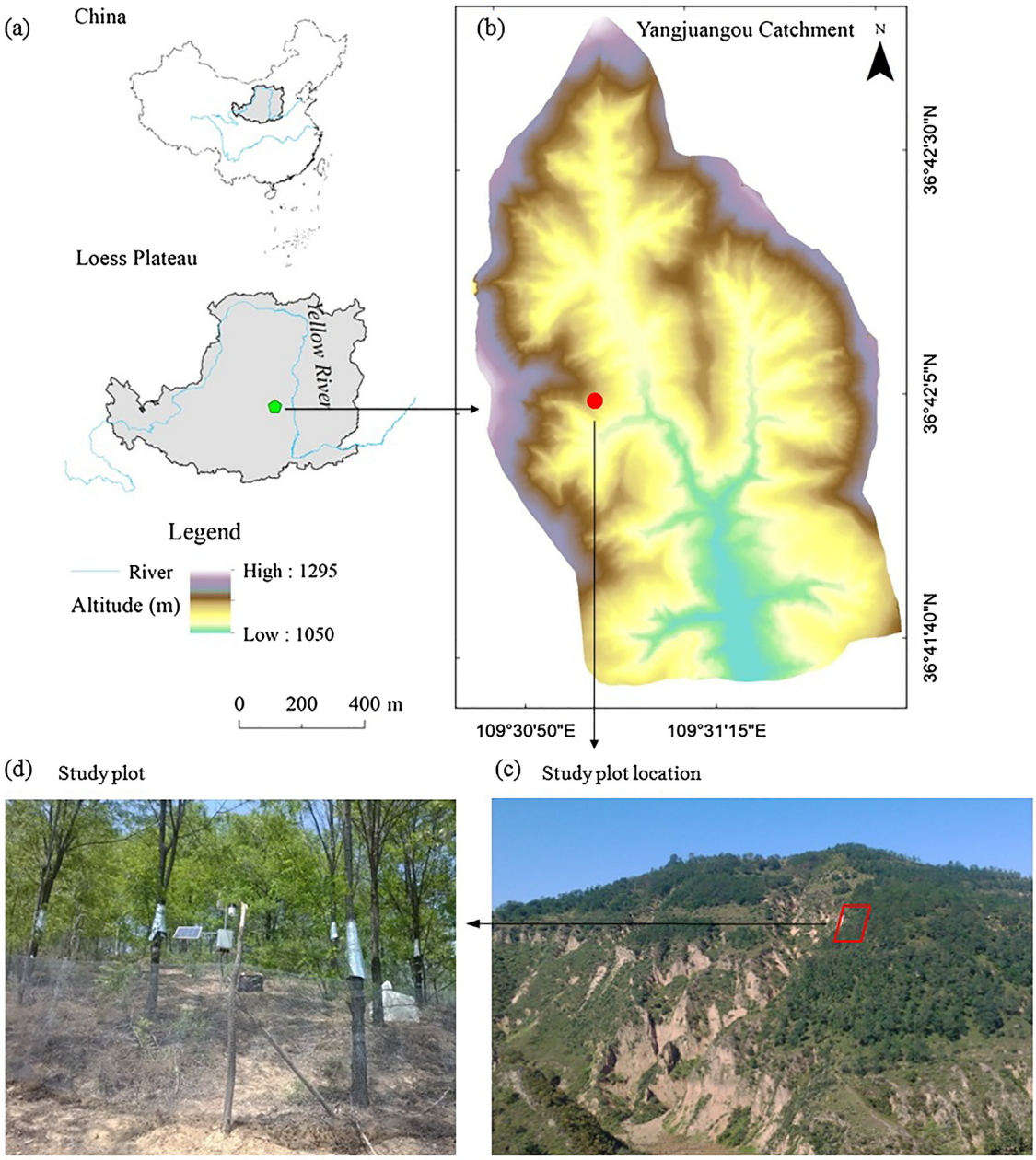

Fig. 1. Location of the study site (a, b and c) and maps of the black locust plantation with sap flow sensors (d) in the Yangjuangou catchment in the Loess Plateau, China.

density of the plantation is 1300 trees ha^{-1}. The understory vegetation consists of the grass species *Artemisia sacrorum* and *Periploca sepium*, which have a mean cover of 25% (Fig. 1d). The canopy cover is approximately 0.80 on this plantation. The monthly leaf area index (LAI) of the black locust trees ranged from 1.9 in September 2016 to 2.6 in July 2015 (Fig. 3). The mean field capacity was 0.161 $m^3 m^{-3}$ and the mean wilting point was 0.058 $m^3 m^{-3}$ in the soil profile from the study stand, and these values were derived from the soil water retention curve.

2.2. Sap flow measurements

In two consecutive growing seasons in 2015 and 2016, thermal dissipation probes (TDP) were used to measure the sap flux density (F_d, $m^3 m^{-2} s^{-1}$) in six trees (Table 1). The TDP consisted of two needles at 10 mm in length and 1.2 mm in diameter. The upper needle was a heater, and the below needle was a reference. The probes contained a copper-constantan thermocouple junction supplied with 1.5 W of power. To install the probes, a 4-cm-wide and 10-cm-tall section of bark from the stem was removed at a height of 1.3 m above ground level. The needles were inserted into the sapwood at the north aspect of the stem. Reflective bubble wrap was wrapped around the tree stem where the TDP probe was installed to prevent the sun from shining on the measured area. The temperature difference between the needles was sampled every 60 s and recorded every 30 min with a data logger (CR1000, Campbell Scientific, Logan, UT, USA). The F_d was calculated based on the temperature difference between the needles using the formula established by Granier (1987). The stand sap flux density (J_s, kg m^{-2} day^{-1}) was calculated with the following formula:

$$J_s = \frac{\sum F_{di} \times A_{si}}{A_s} \quad (1)$$

where F_{di} is the mean value F_d of the measured trees in the i_{th} DBH class and A_{si} is the sum of the tree sapwood area in the i_{th} DBH class.

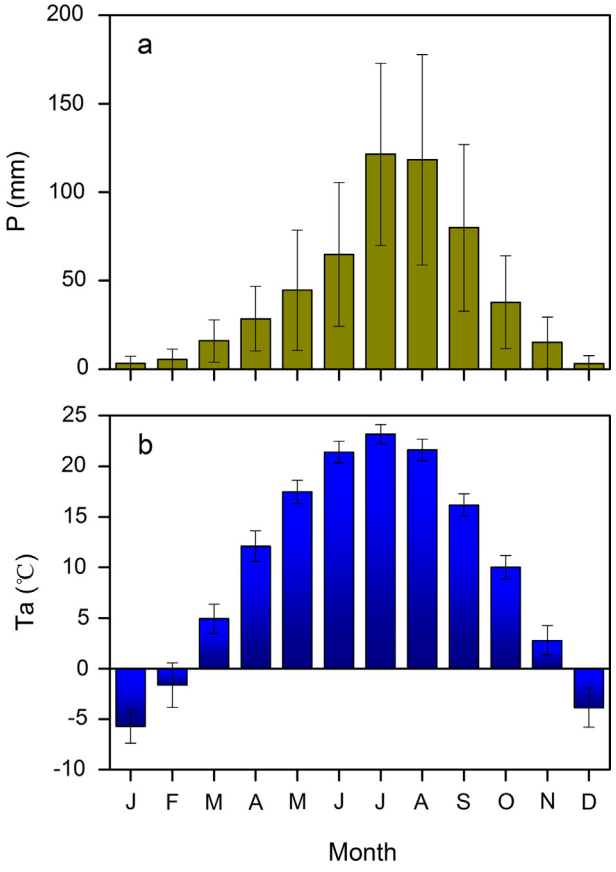

Fig. 2. Multi-year (1952–2012) monthly precipitation (P, mm) (a) and air temperature (Ta, °C) (b) in the study area.

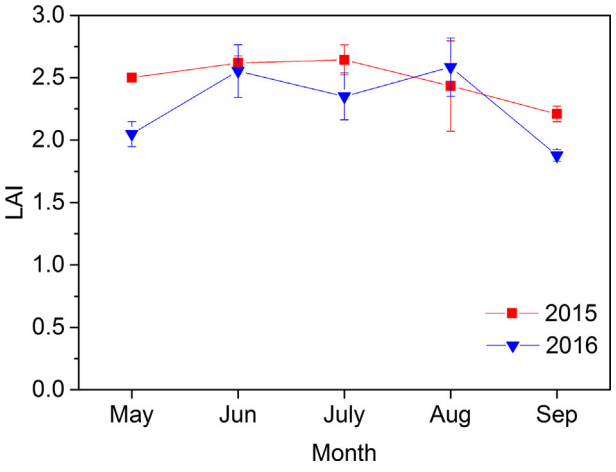

Fig. 3. Dynamics of the monthly tree leaf area index (LAI) during the growing seasons in 2015 and 2016. The LAI was observed three times each month using a Canopy Analyser (LAI-2000, Li-Cor, Lincoln, NE, USA).

Stand transpiration (Tr, mm day^{-1}) was calculated as follows:

$$Tr = \frac{J_s \times A_{ST}}{A_G} \quad (2)$$

where A_{ST} (m^2) is the total sapwood area and A_G (m^2) is the total ground area of the plot.

The sapwood area of the tree (A_s, cm^2) was calculated according the regression formula between A_s and diameter at breast height (1.3 m) above ground (DBH, cm) ($A_s = 0.61 \times DBH^{1.55}$, $R^2 = 0.94$, $n = 22$), which was established based on tree core samples from 22 trees adjacent to the study plot (Jiao et al., 2018). Calibration was conducted according to Jiao et al. (2016b) if the sapwood thickness was less than the needle length.

Table 1
Biometrics in the black locust plantation.

No	[a] DBH/cm	Height/m	Sapwood area/cm^2	Sensors
1	4.6	5.4	6.4	
2	5.9	5.7	9.4	
3	7.5	7.9	13.7	Sapflow (TDP)
4	7.9	9.1	14.8	
5	9.2	8.2	18.8	Sapflow (TDP)
6	10.3	10.5	22.3	
7	10.7	10.6	23.7	Sapflow (TDP)
8	12.3	9.5	29.4	Sapflow (TDP)
9	14.7	10.7	38.7	
10	15.7	10.1	42.9	
11	15.9	10.8	43.7	Sapflow (TDP)
12	16.1	11.2	44.6	
13	17.1	11.5	48.9	Sapflow (TDP)

[a] The DBH of trees in the study plot was measured at the beginning of growing season in 2015.

2.3. Meteorological variables and soil water measurements

Meteorological variables were simultaneously monitored with the sap flow measurements. An automatic weather station was installed in the open area of the catchment at nearly 500 m from the study plot. Air temperature (Ta, °C) and relative humidity (RH, %) were monitored using a HMP35C sensor (Vaisala Co., Helsinki, Finland). The vapor pressure deficit (VPD, kPa) was calculated using Ta and RH data. The wind speed and wind direction were monitored with a wind sentry (03001). Solar radiation (Rs, W m^{-2}) was measured using a pyranometer (Li-200, Li-Cor, Lincoln, NE). The above three instruments were all installed 2 m above ground level. Precipitation (P, mm) was measured using a tipping bucket rain gauge (TE525, Texas Electronics Inc., Dallas, TX, USA). These data were recorded every 30 min with a data logger (CR1000, Campbell Scientific, Logan, UT, USA).

In the study plot, EC-5 sensors (Decagon Devices Inc., Pullman, WA, USA) were used to measure the volumetric soil water content (SWC, m^3 m^{-3}) at various soil depths (10, 20, 40, 60, 80, 100, 120, 150 and 180 cm). Data were recorded at 30-min intervals with a HOBO weather station logger (H21, Onset Computer Corp., Bourne, MA, USA).

The relative extractable soil water (REW) is calculated as follows:

$$REW = \frac{SWC - SWC_W}{SWC_{FC} - SWC_W} \quad (3)$$

where SWC_W is the wilting point (0.058 m^3 m^{-3}) and SWC_{FC} is the field capacity (0.161 m^3 m^{-3}), and these values were derived from the soil water retention curve.

The FAO Penman-Monteith equation was used to estimate the daily potential evapotranspiration (PET, mm) during the study period according to the following formula (Allen et al., 1998):

$$PET = \frac{0.408 \times \Delta \times (R_n - G) + \gamma \times \left(\frac{900}{T_a + 273}\right) \times u_2 \times (e_s - e_a)}{\Delta + \gamma \times (1 + 0.34 \times u_2)} \quad (4)$$

where Δ is the slope of the saturation water vapor pressure at air temperature Ta (kPa °C^{-1}); R_n is the net radiation (MJ m^{-2}); G is the soil heat flux (MJ m^{-2}), which is assumed to be negligible on a daily scale; γ is the psychrometric constant (kPa °C^{-1}); e_s is the saturation vapor pressure (kPa); e_a is the actual vapor pressure (kPa); u_2 is the mean wind speed (m s^{-1}) at a 2-m height; and Ta is the air temperature at a 2-m height. The input parameters were measured by the automatic weather station.

2.4. Canopy-level stomatal conductance estimation

The canopy-level stomatal conductance (Gs, mm s^{-1}) for the plantation was calculated using a simplified inverted Penman-Monteith equation as follows:

$$Gs = 1000 \times \frac{K_g(Ta) \times Tr}{VPD} \quad (5)$$

where Tr (kg m^{-2} s^{-1}) is the daily stand transpiration of the plantation and K_g (kPa m^3 kg^{-1}) is the conductance coefficient as a function of Ta, which accounts for the temperature effects on the psychrometric constant, latent heat of vaporization, specific heat of air at a constant pressure and air density (Grossiord et al., 2017). K_g can be expressed as follows (Phillips and Oren, 1998):

$$K_g = 115.8 \pm 0.4236 \times Ta \quad (6)$$

To calculate Gs, the thermodynamic variables were based on the average values during daylight hours (Phillips and Oren, 1998). Additionally, Tr was summed over 24 h but divided by daylight hours only (Komatsu et al., 2012). Specifically, daylight hours were assumed to be the period between 6:00 am and 7:00 pm in the Yangjuangou catchment during the growing season for this study. Furthermore, data recorded on rainy days and days with a VPD < 0.2 kPa were excluded (Kumagai et al., 2008).

2.5. Model development

In this study, we used the upper boundary line approach developed by Li et al. (2017b) to establish the Tr-REW-PET model, which provides a feasible method of describing the combined effects of soil water and PET. The boundary line approach is based on the hypothesis that the line connecting the data points at the outer margin of the data depicts the functional dependency between the two factors (Schmidt et al., 2000), namely, Tr and REW. First, the responses of Tr to REW were investigated. The upper boundary line was determined to present the Tr-REW relationship without interference, and it was expressed using the formula as follows (Li et al., 2017b):

$$Tr = Tr_{max} \times (1 - e^{a \times REW}) \quad (7)$$

where Tr_{max} (mm) is the constant maximum of Tr with increasing REW and a is the parameter. Tr_{max} and a could be regressed by the boundary line points according to Schmidt et al. (2000).

In addition, all data were divided into 4 classes at the PET interval of 1 mm day^{-1} (PET ≤ 3, 4 < PET ≤ 5, 5 < PET ≤ 6 and PET > 6) to examine whether the Tr-REW relationship was applicable to the varied PET conditions. The Tr-REW relationships at different PET levels were expressed using the formula (7). The parameters were fit with the data in each PET classes (Li et al., 2017b).

Second, an integrated model for Tr was developed. The relationship between Tr_{max} and the median of the PET (PET_m, mm) at the daily scale in each class was quantified by a nonlinear regression:

$$Tr_{max} = b \times PET_m^2 + c \times PET_m + d \quad (8)$$

where b, c and d are parameters. Tr_{max} is quantified based on the Tr-REW regression in each PET level. In this study, the fitted Tr_{max}-PET_m relationship was as follows (Fig. 4): $Tr_{max} = -0.07 \times PET_m^2 + 0.64 \times PET_m - 0.87$ ($R^2 = 0.99$, n = 4).

To develop a model that reflects the coupling effects of REW and PET on Tr, formula (7) and formula (8) were combined into an integrated model:

$$Tr = (b \times PET^2 + c \times PET + d) \times (1 - e^{a \times REW}) \quad (9)$$

All parameters in the above formula were nonlinearly fit with all available data at the daily scale.

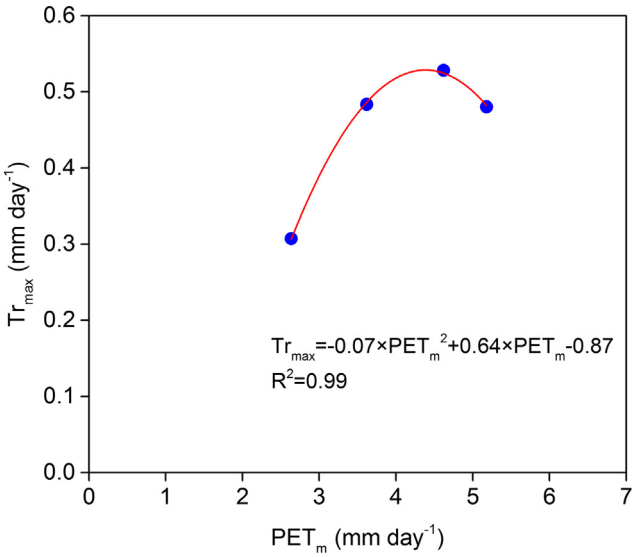

Fig. 4. Relationship between the maximum daily Tr value (Tr_{max}) and median of the daily PET (PET_m) in each PET class.

2.6. Factorial experiments

In this study, the factorial experiment method was used to evaluate the independent contributions of the REW to Tr. The factorial experiment method has been widely used to separate the independent effects of multi-factors on evaporative fluxes (Zhang et al., 2015; Jin et al., 2017). The REW was manipulated and PET varied naturally during the measurements to separate the independent effects of the REW on Tr in this study. First, a controlled Tr model simulation was driven by the lowest REW value (i.e., REW = 0.135, on July 19, 2015) and the PET values measured during the study period:

$$f(control) = (b \times PET^2 + c \times PET + d) \times \left(1 - e^{a \times REW_{min}}\right) \quad (10)$$

where REW_{min} is the minimum REW value observed in the study plot during the study period. Second, the modelled Tr can be calculated using formula (9) and the measured REW and PET values. Third, the difference between the calculated simulation with measured data and the controlled simulation was compared to reflect the impacts of the REW on Tr. Changes in the Tr compared with the controlled Tr (ΔTr) were calculated as follows:

$$\Delta Tr = f(REW) - f(control) \quad (11)$$

where f (REW) is the modelled Tr when the REW is manipulated (i.e., 0.2, 0.3, 0.4, 0.5, 0.6, 0.7, 0.8) and PET is the value observed at the daily scale. The percent change of Tr was calculated as follows:

$$Percent\ change\ of\ Tr = \frac{\Delta Tr}{f(control)} \times 100\% \quad (12)$$

2.7. Statistical analyses

The model simulations of Tr were assessed based on three criteria: root-mean-square error (RMSE), coefficient of determination (R^2) and mean bias (bias).

To analyse the effects of SWC on Gs and determine the controls of Gs on Tr, a logarithmic equation was fitted to Gs and VPD under different SWC classes (Oren et al., 1999):

$$Gs = Gsref - m \times \ln(VPD) \quad (13)$$

where Gsref is the reference conductance at VPD = 1.0 kPa and m describes the sensitivity of Gs to VPD. The parameter Gsref is expected to decline with reduced precipitation and soil moisture, indicating a soil

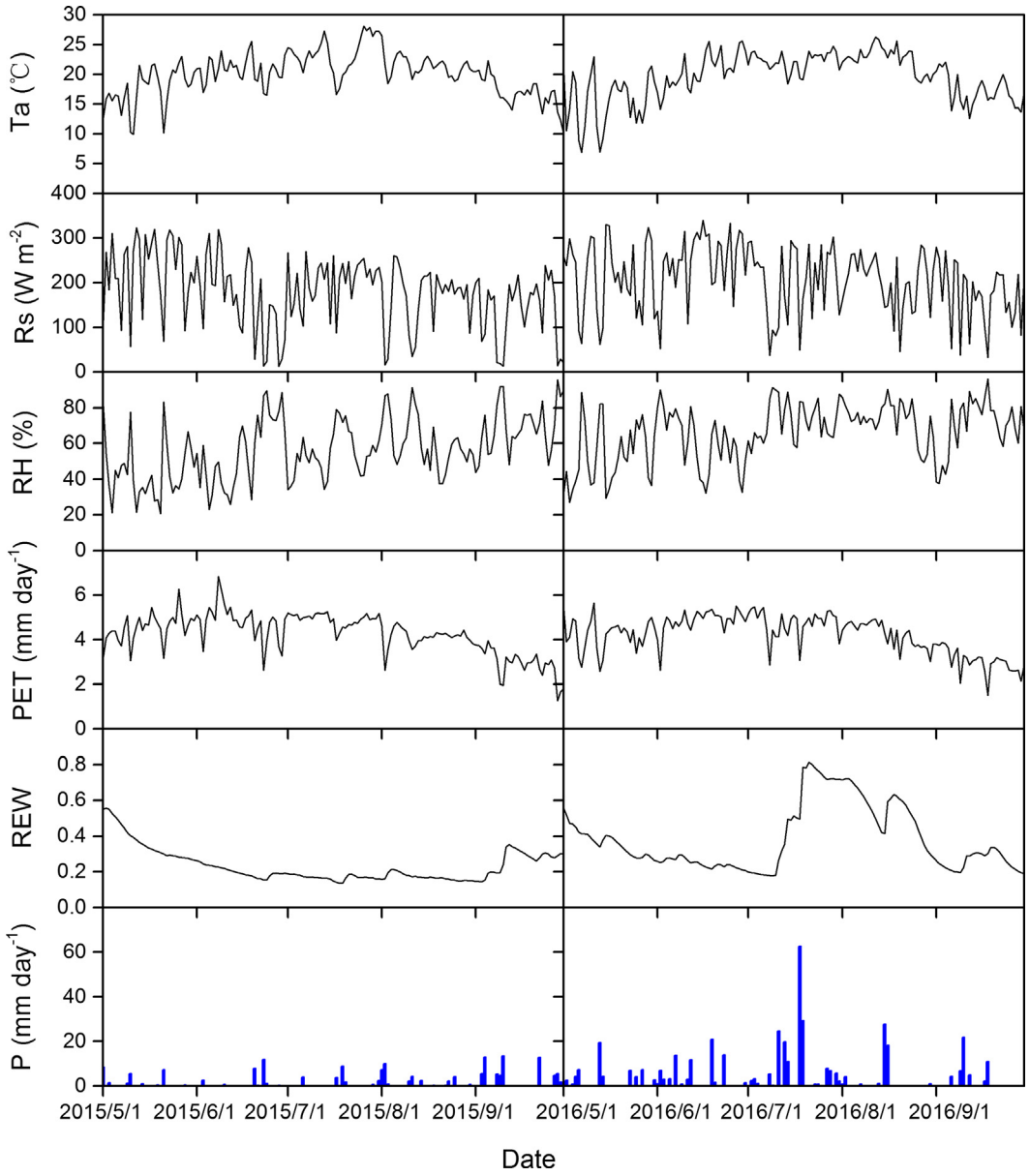

Fig. 5. Daily dynamics of air temperature (Ta, ℃), solar radiation (Rs, W m^{-2}), relative humidity (RH, %), potential evapotranspiration (PET, mm day^{-1}), relative extractable water (REW) at a depth of 0–180 cm and precipitation (P, mm day^{-1}) in the black locust plantation in the Yangjuangou catchment during the 2015 and 2016 growing seasons.

water limitation to Gs (Granier et al., 2000).

All statistical analyses used the SPSS software package (version 11.5 for Windows, SPSS Inc., USA)

3. Results

3.1. Soil water and potential evapotranspiration

During the consecutive growing seasons in 2015 and 2016, the total P was 180.1 mm and 432.6 mm, respectively (Fig. 5). Due to the impact of rainfall, the mean soil water at a depth of 0–180 cm in the 2016 growing season was higher than that in 2015 (Fig. 5), with levels of 0.100 and 0.094 m^3 m^{-3}, respectively. The average daily SWC value had a wide range from 0.086–0.132 m^3 m^{-3} in 2015 and 0.086–0.147 m^3 m^{-3} in 2016. In the vertical profile, the SWC at a depth of 0–100 cm was higher than that in layers deeper than 100 cm (Fig. 6). The temporal dynamic of SWC at a depth of 0–100 cm was tightly related to the pulse of rainfall. The SWC at a depth of 120–180 cm was relatively stable in both the 2015 and 2016 growing seasons, which indicated that deep soil water was rarely impacted by rainfall. The daily PET initially increased and subsequently decreased in each growing season (Fig. 5). The average daily PET was 4.26 mm day^{-1} in 2015 and 4.21 mm day^{-1} in 2016, indicating that the atmospheric demand was relatively lower under humid conditions with abundant rainfall. The daily PET also ranged widely from 6.84 mm to 1.27 mm during the study period.

3.2. Model for transpiration

In both growing seasons, the temporal variations in daily Tr showed a similar trend in which Tr increased at the beginning of the growing season and then declined to the minimal level at the end of the growing season. Tr varied greatly within the growing seasons and ranged from 0.49 mm day^{-1} to 0.03 mm day^{-1} in 2015 and from 0.49 mm day^{-1} to 0.05 mm day^{-1} in 2016. The maximum Tr values occurred on 8 June 2015 and 21 July 2016.

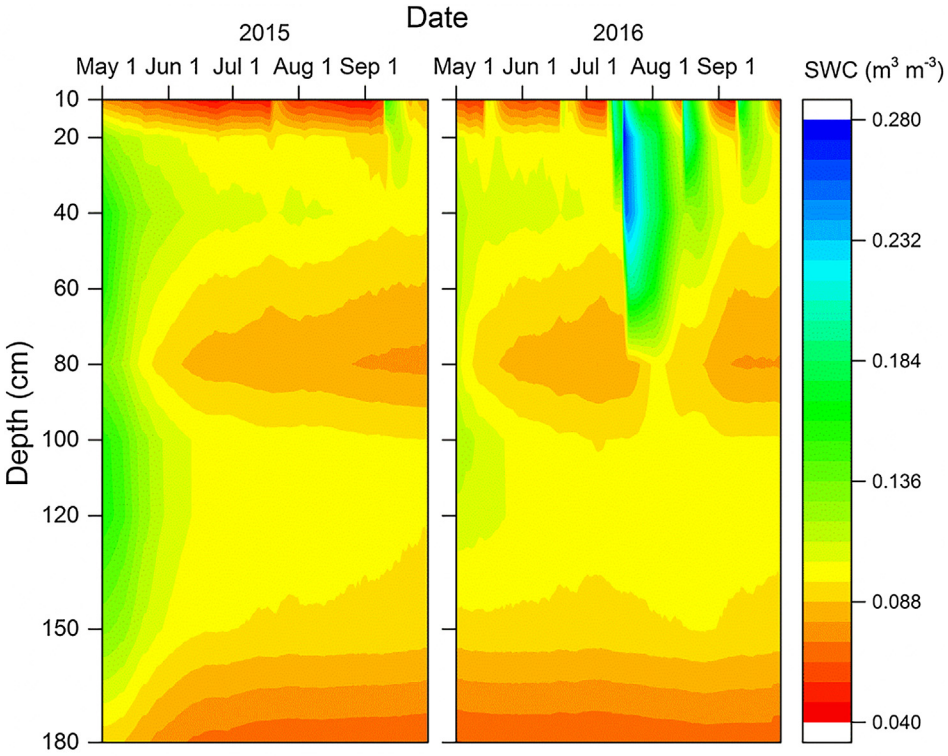

Fig. 6. Temporal and vertical variations of soil water content (SWC, $m^3\ m^{-3}$) in the black locust plantation in the Yangjuangou catchment during the 2015 and 2016 growing seasons.

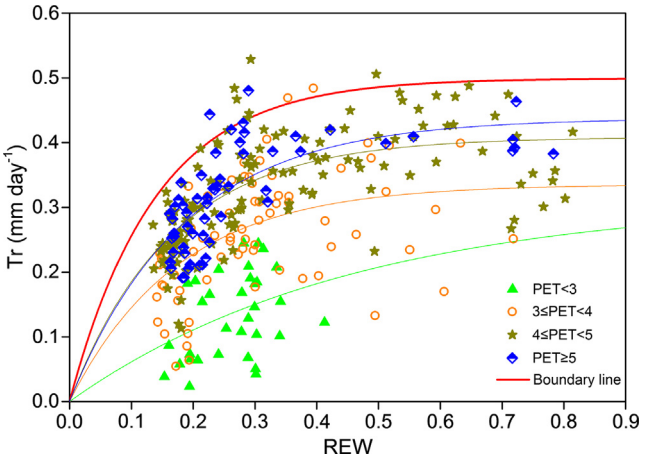

Fig. 7. Boundary line and relationships between the relative extractable water (REW) and transpiration (Tr) of the black locust plantation at varied potential evapotranspiration (PET) levels.

Table 2
Regressions of transpiration (Tr) and relative extractable soil water (REW) relationship for boundary line and each PET levels.

	Regression	R^2	n
Boundary line	$Tr = 0.50 \times (1 - e^{-5.67 \times REW})$	0.69	15
PET < 3	$Tr = 0.27 \times (1 - e^{-2.65 \times REW})$	0.15	33
3 ≤ PET < 4	$Tr = 0.34 \times (1 - e^{-7.20 \times REW})$	0.30	74
4 ≤ PET < 5	$Tr = 0.41 \times (1 - e^{-6.05 \times REW})$	0.49	140
PET ≥ 5	$Tr = 0.44 \times (1 - e^{-5.40 \times REW})$	0.54	59

The upper boundary line showed that Tr increased as the REW increased during the study period (Fig. 7). The regressions of Tr-REW at varied PET levels showed that R^2 of each regression was higher than 0.30 except for the PET < 3 level (Fig. 7 and Table 2), which is related to the limited available data in the PET < 3 level. These results reflected that the Tr-REW relationship fit almost all levels of PET.

Based on formulas (7)–(9), a model integrating PET and REW for Tr was estimated with the measured data. The model can be expressed as follows:

$$Tr = (0.129 \times PET + 0.106) \times (1 - e^{-11.150 \times REW}) \quad (14)$$

A comparison of the estimated Tr using the above model with the measured Tr generated values of $R^2 = 0.65$, RMSE = 0.06 mm day^{-1}, and bias = −0.005 mm day^{-1} (Fig. 8). These results showed that the model could accurately estimate Tr in the black locust plantation.

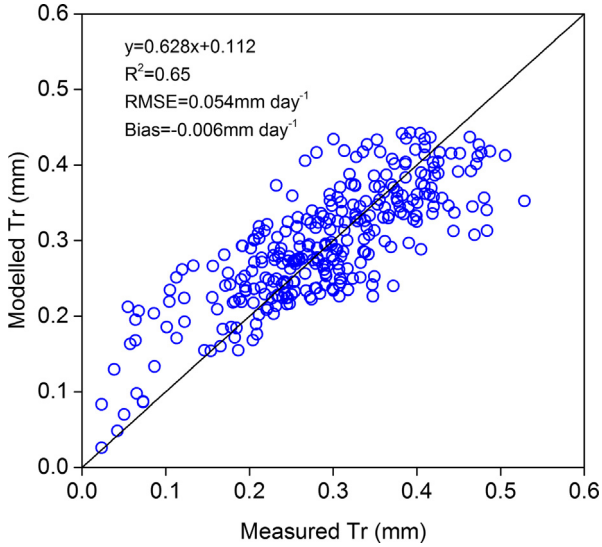

Fig. 8. Relationship between the estimated Tr using the model (modelled Tr, mm) and measured Tr (mm) in the black locust plantation.

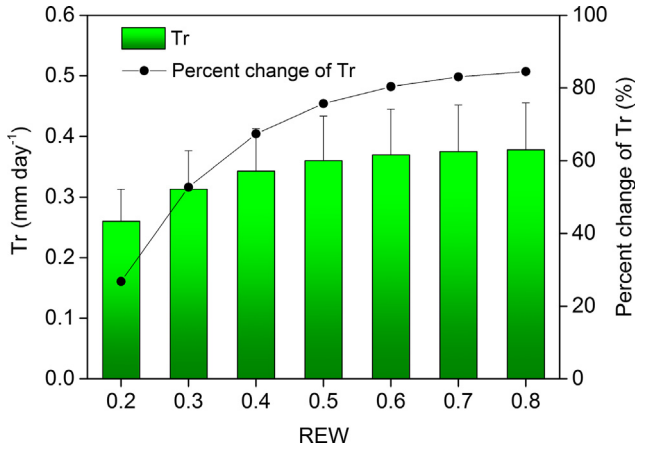

Fig. 9. Percent change of Tr due to the effects of SWC on Tr at different REW levels.

3.3. Effects of REW on Tr

Tr increased sharply with REW when the REW value was less than a threshold of 0.4. As the REW increased beyond the threshold, Tr increased slowly and reached a maximum. The increasing rate of Tr with REW within the threshold (0.4) was 0.53 mm day^{-1} per 0.1 REW, which was higher than the rate of 0.09 mm day^{-1} per 0.1 REW beyond the threshold (Fig. 9). The controlled Tr was calculated based on the REW at the lowest level (0.135) and PET measured during the study period using formula (14). The total value of the controlled Tr was 62.5 mm for the entire study period. The total value of the modelled Tr as measured REW and PET was 89.8 mm for the whole study period (Table 2). Compared to the controlled Tr (at lowest soil water condition), the total Tr increased by 27.3 mm (43.7%) due to the effects of REW (ranging from 0.14–0.81) during the study period.

3.4. Canopy-level stomatal conductance

The Gs declined as the VPD increased during the entire study period (Fig. 10a). According to formula (13), the relationships between Gs and VPD under various REW levels were established. The Gsref was derived from the Gs-VPD relationships and increased as the REW increased, indicating soil water limitations on Gs (Fig. 10).

4. Discussion

4.1. Establishing the relationship between Tr and SWC

Atmospheric evaporative demand and soil water availability are factors that control forest transpiration. Semi-arid and arid areas feature water storage, which increases the importance of soil water in the control of forest Tr. Therefore, the relationship between soil water and Tr was thoroughly investigated in these water-limited areas. The relationship was directly established based on observations of sapflow and the root zone soil water, which can be expressed as linear, logistic and polynomial functions (Table 3). For example, Ji et al. (2016) found that Tr by the shrub *Nitraria tangutorum* linearly increased with the soil water content in the Badain Jaran Desert of northwestern China. Under the same environmental conditions, Tr presented a polynomial pattern response to soil water for *Haloxylon ammodendron* and *Calligonum mongolicum* (Ji et al., 2016). These results revealed that differences in species characteristic represented one of the possible factors underlying the response patterns of Tr to soil water. Studies have also shown that Tr presents a logistic type response to soil water (Lagergren and Lindroth, 2002; Chang et al., 2014). However, other studies have shown that a clear and strong relationship between Tr and soil water cannot be easily established based on field data from multiple forests (Kumagai et al., 2008; Ghimire et al., 2014), which was possibly due to several reasons. First, the water source for plant uptake is determined by the distribution of roots and soil moisture in the soil profile, although the soil water was highly spatially and temporally heterogeneous in forests (Kume et al., 2007; Brito et al., 2015). For example, tree water uptake occurred in the deep soil layers as the drought length increased, and the limited root depth could even result in a negative response of Tr to moist soil conditions (Bréda et al., 1995). Kumagai et al. (2008) also implied that a clear relationship could not be established between Tr and soil water because of the water uptake that occurred in the deep soil layers. However, deep soil moisture was not continuously monitored in these studies. Second, researchers have generally believed that Tr is driven by PET but limited by soil water (Li et al., 2017b). However, it is difficult to disentangle the relative impacts of soil water from environmental factors because they are mostly correlated (Grossiord et al., 2017). For example, Zhao et al. (2006) found that Tr was primarily controlled by PET under higher soil water conditions but that Tr was limited by REW when the soil water declined to a low level in an *Acacia mangium* forest.

In this study, to examine the independent effects of soil water on Tr, we have considered both the soil water in the whole soil zone and the PET conditions. More than 90% of the fine roots are concentrated in the 2-m soil profile (Li et al., 2005). Therefore, we detected the temporal

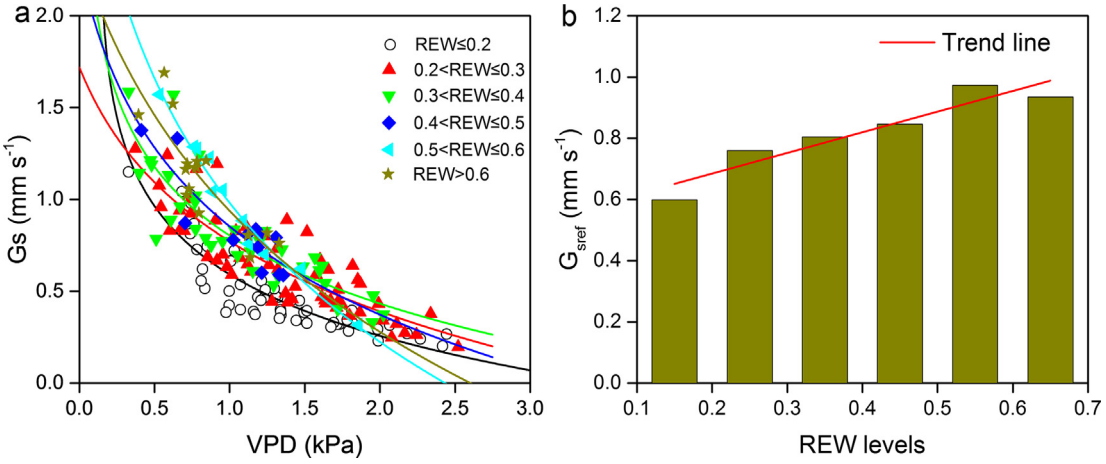

Fig. 10. Relationships between the Gs and VPD at different REW levels (a) and changes in Gsref as the REW increased (b) in the black locust plantation.

Table 3
Response patterns of transpiration (Tr) to soil water in several other studies.

Response pattern of Tr to soil water	Species	Study area	MAP or P during the study period (mm)	Source
Linear pattern	*Nitraria tangutorum*	Badain Jaran Desert of northwestern China	123.5	Ji et al. (2016)
Logistic pattern	*Pinus sylvestris* L.	Norunda forest in central Sweden	270 (from December to April)	Lagergren and Lindroth (2002)
	Picea abies (L.) Karst	Norunda forest in central Sweden	270 (from December to April)	Lagergren and Lindroth (2002)
	Caragana korshinskii	Liudaogou catchment in the north of Loess Plateau, China	437	She et al. (2012)
	Picea crassifolia	Pailougou watershed in the upper Heihe River Basin of northwestern China	290.2–467.8	Chang et al. (2014)
Polynomial pattern	*Nitraria sphaerocarpa*	Desert-oasis ecotone in the middle of China's Heihe River Basin of northwestern China	116.8	Zhao and Liu (2010)
	Elaeagnus angustifolia	Desert-oasis ecotone in the middle of China's Heihe River Basin of northwestern China	116.8	Zhao and Liu (2010)
	Haloxylon ammodendron	Badain Jaran Desert of northwestern China	123.5	Ji et al. (2016)
	Calligonum mongolicum	Badain Jaran Desert of northwestern China	123.5	Ji et al. (2016)

variations and spatial distributions of soil water in the entire root zone in the black locust plantation. The spatial and temporal variations in SWC were evident during the study period (Figs. 5 and 6). Moreover, following the investigation method of Li et al. (2017b) for the coupling effects of PET and REW on Tr in a larch plantation in northwestern China, we developed a model for Tr with PET and REW to accurately estimate Tr in black locust plantations (Fig. 7). More importantly, the model provided a method for examining the REW-Tr relationship with continuous field data.

4.2. Effects of REW on Tr

Based on the model, we found that Tr in the black locust plantation might increase with increasing soil water under unchanged evaporative demand (Fig. 7). The parameter Gsref is expected to decline with reduced precipitation and soil moisture, indicating a soil water limitation to Gs (Granier et al., 2000). Therefore, in this study, Gsref was used to analyse the variation in the stomatal controls on Tr among different soil water conditions. Novick et al. (2016) found that the Gsref for different vegetation increased with increasing soil water. Tr was strongly limited by the soil moisture when soil water deficits occurred. The possible reason for the observed decrease in Tr with soil drying is related to the decline in Gsref during soil water depletion (Fig. 10). Stomatal conductance closure occurs to avoid hydraulic system failure when soil moisture drops with relatively unchanged PET (Oren et al., 1999; Grossiord et al., 2017), and this represents an important mechanism in plants under drought conditions (Novick et al., 2016). In this study, the dynamics of Tr under various SWC conditions were similar to the dynamics of Gsref, which indicated that Gs tightly regulated Tr in the black locust plantation. The stomata closure resulted in a decline in Tr as the soil water decreased in the black locust plantation.

4.3. Prediction of Tr responses to climate change in this region

The spatial and temporal variation in ET has been widely investigated under changes in vegetation and climate in the Loess Plateau (Feng et al., 2012; Jin et al., 2017), and the results have provided implications for ecological restoration and water resource management (Feng et al., 2016). As a dominant component of ET, Tr and its temporal dynamics have not been extensively studied in this region. In contrast, soil water has been widely monitored using different methods (including field observation and remote sensing) at different temporal and spatial scales in this region (Wang et al., 2010; Feng et al., 2017). Our results have provided an approach to predicting the dynamics of Tr in black locust plantations under different soil water conditions based on soil water data.

The effects of climate change will lead to altered precipitation patterns as well as increased temperature in many regions of the world (Grossiord et al., 2017). Soil water stress is expected to worsen due to the combined effects of low precipitation and warming. Precipitation decreased at a rate of 0.99 mm yr^{-1} and the temperature increased annually by an average of 0.02 °C from 1951–2008 in the Loess Plateau (Lü et al., 2012), indicating a warmer and drier climate over the past several decades. The drought frequency and severity in this region are increasing as a result of global warming (Sun et al., 2015; Liu et al., 2019), which could increase stress to forests because of the associated reduction in soil water availability and changes in atmospheric evaporative demand (VPD). In this study, our results implied that Tr in the black locust plantation could decrease with increasing drought under climate change conditions. Consequently, the carbon acquisition and growth of the black locust trees could also be suppressed. Novick et al. (2016) emphasized that the atmospheric evaporative demand, which is directly related to VPD, is increasingly important for ecosystem water and showed that carbon fluxes and hydrological cycles changed due to stomatal closure under increasing VPD. Extreme precipitation events have occurred frequently in this region in recent years. Li et al. (2017a)

found that extremely high precipitation was tightly correlated with El Nino events and occurred in the year following El Nino events. For example, the total rainfall in Yan'an in 2013 was 959 mm, which was much higher than the mean annual precipitation from 1951–2012 (530 mm) (Li, 2017). Although extreme precipitation events could have induced severe soil erosion, landslides and damage to dams (Cao et al., 2015; Wei et al., 2015), the soil water storage was adequately recharged. Our results indicated that transpiration from the black locust plantation would increase with soil water recharge; thus, more water could diffuse to atmosphere from soil through plants, which contributes to evapotranspiration. Additionally, the increased rate of Tr would decrease with increases in soil water. Therefore, the response of transpiration and soil water to extreme precipitation events should be clarified in the future.

5. Conclusions

Forest transpiration is driven by PET and limited by soil water. Due to PET and soil water occurring concurrently under natural conditions, it is difficult to disentangle the independent effects of soil water on Tr. In this study, we developed a method of estimating the independent impact of soil water on forest Tr based on data from continuous observations. Using the upper boundary line method, a Tr model that integrates PET and REW was established, and it was well fit to almost all PET levels. To examine the independent effects of soil water on Tr, the REW was manipulated while the PET varied naturally during the measurements, and the integrated Tr model showed that Tr increased with increasing REW during study period. The rate of Tr increase within a REW threshold (0.53 mm day^{-1} per 0.1 REW) was higher than that beyond the threshold (0.09 mm day^{-1} per 0.1 REW). Under the natural PET condition, Tr increased by 43.7% due to the effects of increasing REW compared to the lowest REW during the study period. This response pattern of Tr to soil water was mainly controlled by canopy stomatal conductance due to its cessation under dry soil conditions. Our study provides a feasible method of investigating the response pattern of Tr to soil water and accurately quantifying the independent contributions (43.7%) of soil water on forest Tr based on field data. In the future, the manner in which forest Tr and soil water in this region respond to extreme precipitation events should be extensively investigated.

Acknowledgements

This study was financially supported by the National Key Research and Development Program of China, China, (No. 2016YFC0501602), the National Natural Science Foundation of China, China (Nos. 41701021, 41571503 and 41771118), and the Fundamental Research Funds by the Central Universities (No. GK201903070). We are grateful to Jianbo Liu and Jianye Li for assistances on the field work.

References

Alcorn, P.J., Forrester, D.I., Thomas, D.S., James, R., Smith, R.G.B., Nicotra, A.B., Bauhus, J., 2013. Changes in whole-tree water use following live-crown pruning in young plantation-grown Eucalyptus pilularis and Eucalyptus cloeziana. Forests 4, 106–121. https://doi.org/10.3390/f4010106.

Allen, C.D., Breshears, D.D., McDowell, N.G., 2015. On underestimation of global vulnerability to tree mortality and forest die-off from hotter drought in the Anthropocene. Ecosphere 6, 1–55. https://doi.org/10.1890/ES15-00203.1.

Allen RG, Pereira LS, Raes D, Smith M. 1998. Crop evapotranspiration - Guidelines for computing crop water requirements - FAO Irrigation and drainage paper 56, FAO, Rome, Italy. In. FAO Rome.

Angstmann, J.L., Ewers, B.E., Barber, J., Kwon, H., 2013. Testing transpiration controls by quantifying spatial variability along a boreal black spruce forest drainage gradient. Ecohydrology 6, 783–793. https://doi.org/10.1002/eco.1300.

Angstmann, J.L., Ewers, B.E., Kwon, H., 2012. Size-mediated tree transpiration along soil drainage gradients in a boreal black spruce forest wildfire chronosequence. Tree Physiol. 32, 599–611. https://doi.org/10.1093/treephys/tps021.

Bréda, N., Granier, A., Barataud, F., Moyne, C., 1995. Soil water dynamics in an oak stand. Plant Soil 172, 17–27. https://doi.org/10.1007/BF00020856.

Brito, P., Lorenzo, J.R., Gonzalez-Rodriguez, A.M., Morales, D., Wieser, G., Jimenez, M.S., 2015. Canopy transpiration of a semi arid Pinus canariensis forest at a treeline ecotone in two hydrologically contrasting years. Agricul. Forest Meteorol. 201, 120–127. https://doi.org/10.1016/j.agrformet.2014.11.008.

Cao, B., Jiao, J., Wang, Z., Wei, Y., Li, Y., 2015. Characteristics of Landslide under the extreme rainstorm in 2013 in the Yanhe Basin. Res. Soil Water Conserv. 22, 103–109. https://doi.org/10.13869/j.cnki.rswc.20151116.015.

Chang, X.X., Zhao, W.Z., He, Z.B., 2014. Radial pattern of sap flow and response to microclimate and soil moisture in Qinghai spruce (Picea crassifolia) in the upper Heihe River Basin of arid northwestern China. Agricult. For. Meteorol. 187, 14–21. https://doi.org/10.1016/j.agrformet.2013.11.004.

Du, S., Wang, Y.L., Kume, T., Zhang, J.G., Otsuki, K., Yamanaka, N., Liu, G.B., 2011. Sapflow characteristics and climatic responses in three forest species in the semiarid Loess Plateau region of China. Agricult. For. Meteorol. 151, 1–10. https://doi.org/10.1016/j.agrformet.2010.08.011.

Dymond, S.F., Bradford, J.B., Bolstad, P.V., Kolka, R.K., Sebestyen, S.D., DeSutter, T.M., 2017. Topographic, edaphic, and vegetative controls on plant-available water. Ecohydrology 10, e1897. https://doi.org/10.1002/eco.1897.

Fang, W., Lu, N., Zhang, Y., Jiao, L., Fu, B., 2017. Responses of nighttime sap flow to atmospheric and soil dryness and its potential roles for shrubs on the Loess Plateau of China. J. Plant Ecol. rtx042. https://doi.org/10.1093/jpe/rtx042.

Feng, X., Fu, B., Piao, S., Wang, S., Ciais, P., Zeng, Z., Lu, Y., Zeng, Y., Li, Y., Jiang, X., Wu, B., 2016. Revegetation in China' s Loess Plateau is approaching sustainable water resource limits. Nat. Climate Change 6, 1019–1022. https://doi.org/10.1038/nclimate3092.

Feng, X., Li, J., Cheng, W., Fu, B., Wang, Y., Lü, Y., Ma, Shao, 2017. Evaluation of AMSR-E retrieval by detecting soil moisture decrease following massive dryland re-vegetation in the Loess Plateau, China. Rem. Sens. Environ. 196, 253–264. https://doi.org/10.1016/j.rse.2017.05.012.

Feng, X.M., Sun, G., Fu, B.J., Su, C.H., Liu, Y., Lamparski, H., 2012. Regional effects of vegetation restoration on water yield across the Loess Plateau, China. Hydrol. Earth Syst. Sci. 16, 2617–2628. https://doi.org/10.5194/hess-16-2617-2012.

Fisher, R., Williams, M., Costa, D., Lola, A., Malhi, Y., da Costa, R., Almeida, S., Meir, P., 2007. The response of an Eastern Amazonian rain forest to drought stress: results and modelling analyses from a throughfall exclusion experiment. Global Change Biol. 13, 2361–2378. https://doi.org/10.1111/j.1365-2486.2007.01417.x.

Fu, B., Wang, S., Liu, Y., Liu, J., Liang, W., Miao, C., 2017. Hydrogeomorphic ecosystem responses to natural and Anthropogenic changes in the Loess Plateau of China. Ann. Rev. Earth Planet. Sci. 45, 223–243. https://doi.org/10.1146/annurev-earth-063016-020552.

Ghimire, C.P., Lubczynski, M.W., Bruijnzeel, L.A., Chayarro-Rincon, D., 2014. Transpiration and canopy conductance of two contrasting forest types in the Lesser Himalaya of Central Nepal. Agricult. For. Meteorol. 197, 76–90. https://doi.org/10.1016/j.agrformet.2014.05.012.

Granier, A., 1987. Evaluation of transpiration in a Douglas-fir stand by means of sap flow measurements. Tree Physiol. 3, 309–320. https://doi.org/10.1093/treephys/3.4.309.

Granier, A., Breda, N., Biron, P., Villette, S., 1999. A lumped water balance model to evaluate duration and intensity of drought constraints in forest stands. Ecol. Modell. 116, 269–283. https://doi.org/10.1016/S0304-3800(98)00205-1.

Granier, A., Loustau, D., Breda, N., 2000. A generic model of forest canopy conductance dependent on climate, soil water availability and leaf area index. Ann. For. Sci. 57, 755–765. https://doi.org/10.1051/forest:2000158.

Grossiord, C., Sevanto, S., Borrego, I., Chan, A.M., Collins, A.D., Dickman, L.T., Hudson, P.J., McBranch, N., Michaletz, S.T., Pockman, W.T., 2017. Tree water dynamics in a drying and warming world. Plant, Cell Environ. https://doi.org/10.1111/pce.12991.

Jasechko, S., Sharp, Z.D., Gibson, J.J., Birks, S.J., Yi, Y., Fawcett, P.J., 2013. Terrestrial water fluxes dominated by transpiration. Nature 496, 347–350. https://doi.org/10.1038/nature11983.

Ji, X., Zhao, W., Kang, E., Jin, B., Xu, S., 2016. Transpiration from three dominant shrub species in a desert-oasis ecotone of arid regions of northwestern China. Hydrol. Process. 30, 4841–4854. https://doi.org/10.1002/hyp.10937.

Jia, X., Ma, Shao, Wei, X., Wang, Y., 2013. Hillslope scale temporal stability of soil water storage in diverse soil layers. J. Hydrol. 498, 254–264. https://doi.org/10.1016/j.jhydrol.2013.05.042.

Jiao, L., Lu, N., Fu, B., Gao, G., Wang, S., Jin, T., Zhang, L., Liu, J., Zhang, D., 2016a. Comparison of transpiration between different aged black locust (*Robinia pseudoacacia*) trees on the semi-arid Loess Plateau, China. J. Arid Land 8, 604–617. https://doi.org/10.1007/s40333-016-0047-2.

Jiao, L., Lu, N., Fu, B., Wang, J., Li, Z., Fang, W., Liu, J., Wang, C., Zhang, L., 2018. Evapotranspiration partitioning and its implications for plant water use strategy: evidence from a black locust plantation in the semi-arid Loess Plateau, China. For. Ecol. Manage. 424, 428–438. https://doi.org/10.1016/j.foreco.2018.05.011.

Jiao, L., Lu, N., Sun, G., Ward, E.J., Fu, B., 2016b. Biophysical controls on canopy transpiration in a black locust (*Robinia pseudoacacia*) plantation on the semi-arid Loess Plateau, China. Ecohydrology 9, 1068–1081. https://doi.org/10.1002/eco.1711.

Jin, Z., Liang, W., Yang, Y., Zhang, W., Yan, J., Chen, X., Li, S., Mo, X., 2017. Separating vegetation greening and climate change controls on evapotranspiration trend over the Loess Plateau. Scientific Reports 7, 8191. https://doi.org/10.1038/s41598-017-08477-x.

Komatsu, H., Onozawa, Y., Kume, T., Tsuruta, K., Shinohara, Y., Otsuki, K., 2012. Canopy conductance for a Moso bamboo (Phyllostachys pubescens) forest in western Japan. Agricult. For. Meteorol. 156, 111–120. https://doi.org/10.1016/j.agrformet.2012.01.004.

Kreuzwieser, J., Rennenberg, H., 2014. Molecular and physiological responses of trees to waterlogging stress. Plant Cell Environ. 37, 2245–2259. https://doi.org/10.1111/pce.12310.

Kumagai, T., Tateishi, M., Miyazawa, Y., Kobayashi, M., Yoshifuji, N., Komatsu, H., Shimizu, T., 2014. Estimation of annual forest evapotranspiration from a coniferous plantation watershed in Japan (1): water use components in Japanese cedar stands. J. Hydrol. 508, 66–76. https://doi.org/10.1016/j.jhydrol.2013.10.047.

Kumagai, T., Tateishi, M., Shimizu, T., Otsuki, K., 2008. Transpiration and canopy conductance at two slope positions in a Japanese cedar forest watershed. Agricult. For. Meteorol. 148, 1444–1455. https://doi.org/10.1016/j.agrformet.2008.04.010.

Kume, T., Takizawa, H., Yoshifuji, N., Tanaka, K., Tantasirin, C., Tanaka, N., Suzuki, M., 2007. Impact of soil drought on sap flow and water status of evergreen trees in a tropical monsoon forest in northern Thailand. For. Ecol. Manage. 238, 220–230. https://doi.org/10.1016/j.foreco.2006.10.019.

Lü, Y., Fu, B., Feng, X., Zeng, Y., Liu, Y., Chang, R., Sun, G., Wu, B., 2012. A policy-driven large scale ecological restoration: quantifying ecosystem services changes in the Loess Plateau of China. e31782. PloS One 7. https://doi.org/10.1371/journal.pone.0031782.

Lagergren, F., Lindroth, A., 2002. Transpiration response to soil moisture in pine and spruce trees in Sweden. Agricult. For. Meteorol. 112, 67–85. https://doi.org/10.1016/s0168-1923(02)00060-6.

Li, H., 2017. Cause Analysis of Extreme Rainfall in Yan'an and Study of Unconventional Simulation Test. In. Research Center of Eco-environments and Soil and Water Conservation. Chinese Academy of Sciences & Ministry of Education.

Li, H.J., Gao, J.E., Zhang, H.C., Zhang, Y.X., Zhang, Y.Y., 2017a. Response of extreme precipitation to solar activity and el nino events in typical regions of the loess plateau. Adv. Meteorol. 2017, 1–9. https://doi.org/10.1155/2017/9823865.

Li, P., Zhao, Z., Li, Z., Tan, T., 2005. Characters of root biomass spatial distribution of *Robinia pseudoacacia* in Weibei loess areas. Ecol. Environ. 14, 405–409.

Li, Z., Yu, P., Wang, Y., Webb, A.A., He, C., Wang, Y., Yang, L., 2017b. A model coupling the effects of soil moisture and potential evaporation on the tree transpiration of a semi-arid larch plantation. e1764. Ecohydrology 10. https://doi.org/10.1002/eco.1764.

Liu, Z., Liu, Y., Baig, M.H.A., 2019. Biophysical effect of conversion from croplands to grasslands in water-limited temperate regions of China. Sci. Total Environ. 648, 315–324. https://doi.org/10.1016/j.scitotenv.2018.08.128.

MacKay, S.L., Arain, M.A., Khomik, M., Brodeur, J.J., Schumacher, J., Hartmann, H., Peichl, M., 2012. The impact of induced drought on transpiration and growth in a temperate pine plantation forest. Hydrol. Process. 26, 1779–1791. https://doi.org/10.1002/hyp.9315.

Naithani, K.J., Ewers, B.E., Pendall, E., 2012. Sap flux-scaled transpiration and stomatal conductance response to soil and atmospheric drought in a semi-arid sagebrush ecosystem. J. Hydrol. 464, 176–185. https://doi.org/10.1016/j.jhydrol.2012.07.008.

Novick, K.A., Ficklin, D.L., Stoy, P.C., Williams, C.A., Bohrer, G., Oishi, A.C., Papuga, S.A., Blanken, P.D., Noormets, A., Sulman, B.N., Scott, R.L., Wang, L., Phillips, R.P., 2016. The increasing importance of atmospheric demand for ecosystem water and carbon fluxes. Nat. Clim. Change 6, 1023. https://doi.org/10.1038/nclimate3114.

O'Brien, J.J., Oberbauer, S.F., Clark, D.B., 2004. Whole tree xylem sap flow responses to multiple environmental variables in a wet tropical forest. Plant Cell Environ. 27, 551–567. https://doi.org/10.1111/j.1365-3040.2003.01160.x.

Oren, R., Pataki, D.E., 2001. Transpiration in response to variation in microclimate and soil moisture in southeastern deciduous forests. Oecologia 127, 549–559. https://doi.org/10.1007/s004420000622.

Oren, R., Sperry, J., Katul, G., Pataki, D., Ewers, B., Phillips, N., Schafer, K., 1999. Survey and synthesis of intra-and interspecific variation in stomatal sensitivity to vapour pressure deficit. Plant Cell Environ. 22, 1515–1526. https://doi.org/10.1046/j.1365-3040.1999.00513.x.

Phillips, N., Oren, R., 1998. A comparison of daily representations of canopy conductance based on two conditional time-averaging methods and the dependence of daily conductance on environmental factors. Ann. Des Sci. For. 55, 217–235. https://doi.org/10.1051/forest:19980113.

Poorter, H., Fiorani, F., Stitt, M., Schurr, U., Finck, A., Gibon, Y., Usadel, B., Munns, R., Atkin, O.K., Tardieu, F., 2012. The art of growing plants for experimental purposes: a practical guide for the plant biologist. Funct. Plant Biol. 39, 821–838. https://doi.org/10.1071/FP12028.

Raz-Yaseef, N., Yakir, D., Schiller, G., Cohen, S., 2012. Dynamics of evapotranspiration partitioning in a semi-arid forest as affected by temporal rainfall patterns. Agricult. For. Meteorol. 157, 77–85. https://doi.org/10.1016/j.agrformet.2012.01.015.

Schmidt, U., Thöni, H., Kaupenjohann, M., 2000. Using a boundary line approach to analyze N2O flux data from agricultural soils. Nutri. Cycl. Agroecosyst. 57, 119–129. https://doi.org/10.1023/A:1009854220769.

She, D., Xia, Y., Shao, M., Peng, S., Yu, S., 2012. Transpiration and canopy conductance of Caragana korshinskii trees in response to soil moisture in sand land of China. Agroforest. Syst. 87, 667–678. https://doi.org/10.1007/s10457-012-9587-4.

Shimizu, T., To, Kumagai, Kobayashi, M., Tamai, K., Si, Iida, Kabeya, N., Ikawa, R., Tateishi, M., Miyazawa, Y., Shimizu, A., 2015. Estimation of annual forest evapotranspiration from a coniferous plantation watershed in Japan (2): Comparison of eddy covariance, water budget and sap-flow plus interception loss. J.Hydrol. 522, 250–264. https://doi.org/10.1016/j.jhydrol.2014.12.021.

Sun, W., Song, X., Mu, X., Gao, P., Wang, F., Zhao, G., 2015. Spatiotemporal vegetation cover variations associated with climate change and ecological restoration in the Loess Plateau. Agricult. For. Meteorol. 209–210, 87–99. https://doi.org/10.1016/j.agrformet.2015.05.002.

Ungar, E.D., Rotenberg, E., Raz-Yaseef, N., Cohen, S., Yakir, D., Schiller, G., 2013. Transpiration and annual water balance of Aleppo pine in a semiarid region: implications for forest management. For. Ecol. Manage. 298, 39–51. https://doi.org/10.1016/j.foreco.2013.03.003.

Wang, J., Fu, B., Lu, N., Zhang, L., 2017. Seasonal variation in water uptake patterns of three plant species based on stable isotopes in the semi-arid Loess Plateau. Sci. Total Environ. 609, 27–37. https://doi.org/10.1016/j.scitotenv.2017.07.133.

Wang, Y., Fu, B., Lü, Y., Chen, L., 2011. Effects of vegetation restoration on soil organic carbon sequestration at multiple scales in semi-arid Loess Plateau, China. Catena 85, 58–66. https://doi.org/10.1016/j.catena.2010.12.003.

Wang, Y.Q., Shao, M.A., Liu, Z.P., 2010. Large-scale spatial variability of dried soil layers and related factors across the entire Loess Plateau of China. Geoderma 159, 99–108. https://doi.org/10.1016/j.geoderma.2010.07.001.

Wei, Y., Wang, Z., He, Z., Yu, W., Li, Y., Jiao, J., 2015. Investigation and evaluation on check dams damaged condition under continuous rainstorm in Yanhe River Basin in July 2013. Bull. Soil Water Conservat. 35, 250–255. https://doi.org/10.13961/j.cnki.stbctb.2015.03.052.

Yang, L., Wei, W., Chen, L., Jia, F., Mo, B., 2012. Spatial variations of shallow and deep soil moisture in the semi-arid Loess Plateau, China. Hydrol. Earth Syst. Sci. 16, 3199–3217. https://doi.org/10.5194/hess-16-3199-2012.

Zhang, K., Kimball, J.S., Nemani, R.R., Running, S.W., Hong, Y., Gourley, J.J., Yu, Z., 2015. Vegetation greening and climate change promote multidecadal rises of global land evapotranspiration. Scientific Reports 5, 15956. https://doi.org/10.1038/srep15956.

Zhang, Y., Xu, J., Su, W., Zhao, X., Xu, X., 2018. Spring precipitation effects on formation of first row of earlywood vessels in Quercus variabilis at Qinling Mountain (China). Trees. https://doi.org/10.1007/s00468-018-1792-y.

Zhao, P., Rao, X.Q., Ling, M.A., Cai, X.A., Zeng, X.P., 2006. Sap flow-scaled stand transpiration and canopy stomatal conductance in an Acacia mangium forest. J. Plant Ecol. 30, 655–665. https://doi.org/10.17521/cjpe.2006.0086.

Zhao, W.Z., Liu, B., 2010. The response of sap flow in shrubs to rainfall pulses in the desert region of China. Agricult. For. Meteorol. 150, 1297–1306. https://doi.org/10.1016/j.agrformet.2010.05.012.